

Theory of electric transport through Fe/V/Fe trilayers including the effect of impurities

H. C. Herper^{*1}, L. Szunyogh², and P. Entel¹

¹ Inst. of Physics, University of Duisburg-Essen, Campus Duisburg, D-47048 Duisburg, Germany

² Dept. of Physics, Budapest University of Technology and Economics, H-1521 Budapest, Hungary

Received 1 September 2004

Key words GMR, Kubo-Greenwood equation, Korringa-Kohn-Rostoker method, magnetic properties

PACS 71.15.-m, 75.47.De, 75.70.Cn

The influence of Al and Si impurity layers on the giant magnetoresistance (GMR) and the magnetic properties of Fe/V/Fe(110) trilayers is investigated. The calculations are performed by employing the spin-polarized Kubo-Greenwood approach and the screened Korringa-Rostoker method for layered systems. All calculations are carried out with a fully-relativistic version. Therefore, we are able to consider also anisotropic magnetoresistance effects, which are common in Fe/V systems. We find that the AMR always makes a tiny contribution to the resistivity in alike multilayers so that the magnetoresistance is entirely due to the GMR. A reduction of the GMR due to the Al and Si impurities is observed for current in-plane (CIP) and perpendicular (CPP) geometry. However, in the case of CIP geometry the influence of the impurities decreases with increasing V layer thickness, whereas in the CPP case the difference alternates between 0 and 7%.

Copyright line will be provided by the publisher

1 Introduction

Since, the discovery of the giant magnetoresistance (GMR) in magnetic multilayers [1, 2], this effect has been studied in many systems – both theoretically and experimentally [3, 4, 5]. It describes the dependence of the resistance of two FM layers separated by a nonmagnetic (NM) layer on the relative magnetic configuration of the two ferromagnets. Theoretical and experimental studies have shown that the size of the GMR is not only determined by the choice of the materials, but is sensible to many other parameters, e.g. thickness of the spacer, growth technique, and alloy formation at the interface [6, 7]. Furthermore, the GMR is related to the interlayer exchange coupling of the FM layers and magnetic anisotropy effects, which depend on the orientation of the sample. This implies that the GMR may also vary with the growth direction [8, 9]. An illustrative example can be found in Ref. [10], where the GMR of Fe/Cr_{1-x}V_x multilayers was discussed for two different growth directions. The GMR changes up to 8% for the same spacer thickness but different growth direction.

The applicable GMR can be superimposed by natural resistance effects, e.g. the Lorentz MR in metals or the anisotropic magnetoresistance (AMR), which is a measure for the change of the resistance due to a change of the relative orientation between the electric current and the magnetic field [4]. In experiments with Fe/V_s(110) multilayers a minimum V thickness of $s = 16 \text{ \AA}$ is necessary until the GMR dominates the AMR [8]. In addition, in multilayered structures the GMR can also depend on the thickness of the magnetic layers [11].

In the present paper we study the GMR in Fe/V_s/Fe(110) trilayers, where the V layers are placed between two semi-infinite Fe leads [12], i.e. the thickness of the Fe layers is kept fixed and we focus on the dependence of the GMR on the V thickness. We assume perfect interfaces; alloy formation, which

* Corresponding author: e-mail: heike@thp.uni-duisburg.de, Phone: +49 203 379 3564, Fax: +49 203 379 3665

could reduce the GMR, will be discussed elsewhere [13]. However, additional calculations have been performed for trilayers with an impurity layer at one interface. We use Al and Si impurities, because it has been reported at least for bulk Fe₃V alloys that their magnetic and transport properties are tunable substituting Fe partially by NM atoms like Al and Si [14]. However, we do not consider the Heusler type lattice structure, but embed the impurity layers in the bcc parent lattice [15]. Though, it has been observed in Fe/V multilayers that the AMR can cover the GMR, we will take into account the AMR at least for some selected systems.

2 Computational details

2.1 Structure and self-consistent calculation

Fe/V_s/Fe(110) and Fe/V_s/I₁/Fe(110) (I = {Al, Si}) trilayers are used to study the magnetoresistance behavior in dependence of the V thickness. The possible charge accumulation between spacer and Fe leads is considered by adding n Fe buffer layers on each side of the spacer. The actual systems then consist of $l = 2n + s (+1)$ layers, whereby +1 denotes the Al or Si impurity layer. The investigations of the trilayers are done in two steps. First, the potentials of the ferromagnetic reference configuration $C_0(l)$ are calculated self-consistently for varying V thicknesses s by using the fully-relativistic Screened Korringa-Kohn-Rostoker (SKKR) Green's function method [16, 17]. These potentials are used in the second step to investigate the magnetoresistance of the Fe/V/Fe trilayers, see Sec. 2.2. All calculations are performed within the atomic sphere approximation (ASA). Fe/V superlattices grown on MgO have a bcc-like lattice, with negligible in-plane lattice relaxations [8]. Therefore, we use a bcc parent lattice [15] with a fixed in-plane constant $a = 5.4169$ a.u., i.e. the layer distance is $d_{\perp} = 3.83$ a.u., which corresponds to the experimental lattice constant of bcc Fe.

In the present paper the layers are grown in the $\hat{x} - \hat{y}$ plane, i.e. \hat{z} is perpendicular to the surface. From experiment it is known that the magnetic moments in Fe/V systems are oriented parallel to the plane of layers [18]. This is considered by choosing the magnetic reference configuration $C_0(l)$

$$C_0(l) = \{\overbrace{\hat{\mathbf{x}}, \hat{\mathbf{x}}, \hat{\mathbf{x}}, \dots, \hat{\mathbf{x}}, \hat{\mathbf{x}}}^{l=2n+s(+1)}\}. \quad (1)$$

2.2 Magnetoresistance

The Kubo-Greenwood equation [19, 20, 21] is used to determine the diagonal elements $\sigma_{\mu\mu}$ of the conductivity tensor. For a given magnetic configuration C_{α} and the system length l the conductivity reads

$$\sigma_{\mu\mu}(C_{\alpha}, l, \delta) = \sum_{j,k=1}^l = \sigma_{\mu\mu}^{jk}(C_{\alpha}, \delta), \quad \mu \in \{x, y\}, \quad (2)$$

where $\sigma_{\mu\mu}^{jk}(C_{\alpha}, \delta)$ describes the current in layer j , which is caused by the electric field in layer k . δ is the imaginary part of the complex Fermi-energy $E_F = \epsilon_F + i\delta$, which amounts to 2 mRy in all present calculations and will be left out in the following. A detailed discussion of the influence of δ on the conductivity can be found in Refs. [3, 22]. In the case of CIP geometry the resistivity is given by

$$\rho_{\mu\mu}(C_{\alpha}, l) = (\sigma_{\mu\mu}(C_{\alpha}, l))^{-1}, \quad \mu \in \{x, y\}. \quad (3)$$

The GMR of a layered system is then described by the resistance ratio

$$R = \frac{\rho_{\mu\mu}(C_a, l) - \rho_{\mu\mu}(C_0, l)}{\rho_{\mu\mu}(C_a, l)}, \quad (4)$$

with C_a representing the antiparallel alignment of the Fe layers

$$C_a(l) = \begin{cases} \left\{ \overbrace{\{\hat{\mathbf{x}}, \dots, \hat{\mathbf{x}}\}}^{l/2}, \overbrace{\{-\hat{\mathbf{x}}, \dots, -\hat{\mathbf{x}}\}}^{l/2} \right\} & : l \text{ even} \\ \left\{ \overbrace{\{\hat{\mathbf{x}}, \dots, \hat{\mathbf{x}}\}}^{(l-1)/2}, \overbrace{\{-\hat{\mathbf{x}}, \dots, -\hat{\mathbf{x}}\}}^{(l+1)/2} \right\} & : l \text{ odd.} \end{cases} \quad (5)$$

However, due to anisotropy effects we observe slightly different values for $\rho_{\mu\mu}$ depending on the orientation of the magnetic field, i.e. $B||\hat{\mathbf{x}}$ or $B||\hat{\mathbf{y}}$. Therefore, we make use of a serial resistor model

$$\rho_{||} = \frac{1}{2} \left(\rho_{xx}^{\mathbf{B}||\hat{\mathbf{x}}}(C_\alpha, l) + \rho_{yy}^{\mathbf{B}||\hat{\mathbf{y}}}(C_\alpha, l) \right), \quad \rho_{\perp} = \frac{1}{2} \left(\rho_{xx}^{\mathbf{B}||\hat{\mathbf{y}}}(C_\alpha, l) + \rho_{yy}^{\mathbf{B}||\hat{\mathbf{x}}}(C_\alpha, l) \right). \quad (6)$$

Using $\rho_{||}$ and ρ_{\perp} instead of Eq. (3) the GMR is given by

$$R_d = \frac{\rho_d(C_a, l) - \rho_d(C_0, l)}{\rho_d(C_a, l)}, \quad d = \{||, \perp\}. \quad (7)$$

The anisotropic magnetoresistance (AMR), which describes the dependence of the resistance on the relative orientation of the magnetic field and the current, can easily be obtained from Eq. (6)

$$R_A = \frac{\rho_{||}(C_0, l) - \rho_{\perp}(C_0, l)}{\rho_{av}(C_0, l)}, \quad (8)$$

with $\rho_{av}(C_0, l)$ being the average resistivity, which is in bulk systems defined as $\rho_{av} = \frac{1}{3}(\rho_{||} + 2\rho_{\perp})$. For layered systems with most magnetic moments in-plane one can also use $\rho_{av} = \frac{1}{2}(\rho_{||} + \rho_{\perp})$ [23]. From the theoretical point of view it is convenient to use $\rho_{av} = \rho_{\perp}$, because no domain structure is taken into account.

In the case of CPP geometry the resistivity can not be obtained from Eq. (2). In this case the electric field along the $\hat{\mathbf{z}}$ -direction is not constant. However, it has been shown that the CPP GMR can at least be described in the steady state [3, 24] by using sheet resistances

$$r(C_\alpha, l) = \sum_{j,k=1}^l \rho^{jk}(C_\alpha, l), \quad (9)$$

where $\rho^{jk}(C_\alpha, l)$ are the layer dependent resistivities, for details see Ref. [3]. The CPP GMR is then given by

$$R_{\text{CPP}} = \frac{r(C_a, l) - r(C_0, l)}{r(C_a, l)}. \quad (10)$$

Similar to Eq. (7) R_{CPP} is calculated for $\mathbf{B}||\hat{\mathbf{x}}$ and $\mathbf{B}||\hat{\mathbf{y}}$.

3 Magnetic properties and GMR

3.1 Magnetic structure

Recent x-ray magnetic circular dichroism measurements (XMCD) and *ab initio* calculations have shown that V layers exhibit induced magnetic moments, which are oriented antiparallel to the magnetic moments of the Fe layers [25, 18, 26]. This is also observed in the present trilayers. In Fig. 1 the total magnetic moments, i.e. sum of spin- and orbital moments, for $s = 8$ are shown. In agreement with Coehoorn [26] the largest magnetic moments can be found at the interfaces. With increasing distance from the interface

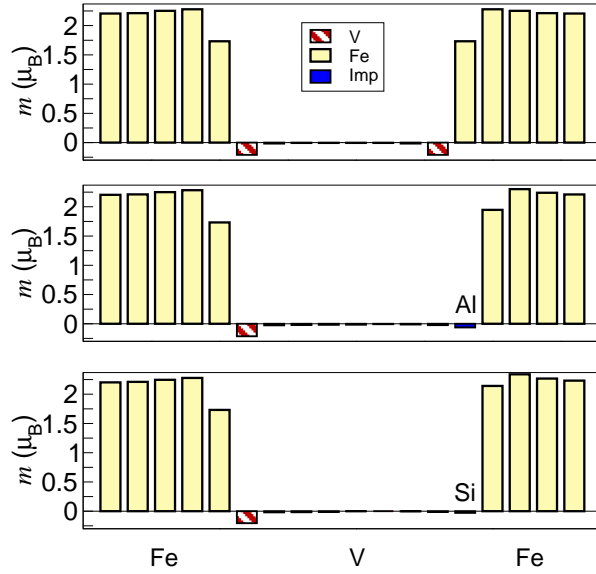


Fig. 1 Layer resolved magnetic moments m of Fe/V $_s$ /Fe and Fe/V $_s$ /I $_1$ /Fe ($I \in \{\text{Al}, \text{Si}\}$). Light bars denote the magnetic moments of the 4 or 5 Fe buffer layers being closest to the V spacer. The outer Fe layers, which are not shown, have a bulk-like magnetic moment. The m of the V layers (hatched bars) and the impurity layers (dark bars) are anti-parallel aligned to the magnetic moments of Fe.

the moments diminish, such that the magnetic moments of the layers in the center are usually by one or two orders of magnitude smaller as compared to the interface layers, which is in agreement with the experimental findings [18]. The magnetic moments of the Fe layers at the interfaces are reduced as compared to the bulk value.

Similar observations are made for the systems with impurities, but the induced magnetic moments of V become smaller at the Fe/Si and Fe/Al interface, respectively, because the impurities shield the spacer from the Fe layers. This means the the size of the magnetic moments is sensible to the type of the interface, but it is nearly independent from the size of the spacer s , Fig. 2. From $s = 4$ the interface moments amount to $m \approx 0.21 \mu_B/\text{interface}$ for Fe/V/Fe trilayers being in agreement with Ref. [26]. However, the *ab initio* calculated moments seem to be smaller than the value obtained from XMCD measurements [18] ($0.45 - 1 \mu_B$). Magnetic moments of comparable size to the results of Wende *et al.* [18] are achieved if we include some kind of disorder, e.g. a two-layer interdiffusion at the interfaces [13]. For systems with 10 % intermixing the magnetic moments of the outer V layers m_V^{int} amount to $\approx 0.6 \mu_B$; consequently, one can guess that there might be interdiffusion in Ref. [18].

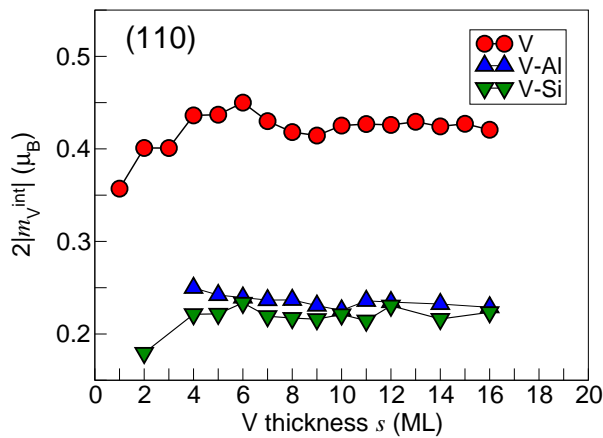


Fig. 2 Magnetic moments m_V^{int} of the two outermost V layers for Fe/V $_s$ /Fe (circles) and Fe/V $_s$ /I $_1$ /Fe ($I \in \{\text{Al}, \text{Si}\}$) (triangles) vs. the spacer thickness s .

3.2 Transport properties

The GMR of the Fe/V/Fe(110) trilayers and the systems including Al or Si impurities are investigated for V thicknesses varying from $s = 1$ to 16. In the CIP case this is done by using Eq. (7). Instead of this for CPP geometry we have to take Eq. (10), where the resistivities in Eq. (3) are replaced by sheet resistances, cf. Eq. (9). In the presence of Si or Al layers we only consider V thicknesses larger than three (one exception is made for Fe/V₂/Si₁/Fe), otherwise Si or Al could not be regarded as impurities. The dependence of the GMR on the V thickness is given in Fig. 3 for both symmetries, whereby only the results for R_{\perp} are shown. This is sufficient, because we observe that the differences between R_{\perp} and R_{\parallel} are always tiny, i.e. $\Delta R \leq 0.2\%$. With increasing spacer thickness the GMR effect becomes smaller for all presented systems,

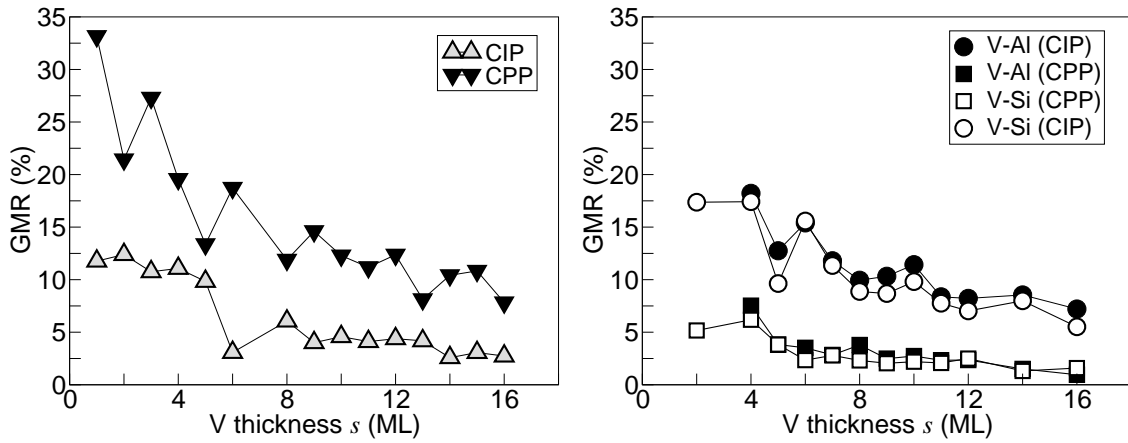


Fig. 3 GMR of Fe/V_s/Fe (left panel) and Fe/V_s/I₁/Fe ($I \in \{\text{Al}, \text{Si}\}$) (right panel) depending on the number of V layers s . The results are given for the magnetic field oriented perpendicular to the electric current. The GMR values are obtained from Eq. (7) (CIP) and Eq. (10) (CPP).

however the slope, i.e. the s dependence, is related to the geometry (CPP or CIP) and to the existence of impurities. The values vary from 33% for CPP geometry and extremely thin V layers in Fe/V_s/Fe to 0.9% for the CIP case containing Al or Si layers. Without impurities the CPP GMR decreases from $s = 1$ on and does not saturate within the considered spacer layer thicknesses. However, if a Si or Al layers are included the CPP GMR curve flattens out for $s > 8$. The CIP GMR develops quite different from the CPP case, because it shows a kind of step-like behavior. For V thicknesses smaller than $s = 4$ the GMR is mainly constant, but the GMR decreases if $4 < s < 8$ is fulfilled. Further increase of the V thickness does not lead to significant changes of the CIP GMR until $s = 14$, where the next step seems to occur. In order to verify this, additional calculations for thicker V spacers have to be done in the future.

It is known that the GMR is mostly caused by the interface region. In order to understand, what causes the step-like decrease, it may be helpful to look for the layer-dependent contributions to the conductivities by carrying out only one summation in Eq. (2)

$$\sigma_{\mu\mu}^k(C_\alpha, l) = \sum_{j=1}^l \sigma_{\mu\mu}^{jk}(C_\alpha, l), \quad \mu \in \{x, y\}. \quad (11)$$

Inverting Eq. (11) appropriate to Eq. (3) one can define the difference of the layer-resolved resistivities

$$\Delta\rho_{\mu\mu}^k(l) = \rho_{\mu\mu}^k(C_\alpha) - \rho_{\mu\mu}^k(C_0), \quad (12)$$

which roughly reflects the contributions of layer k to the GMR. One should keep in mind that only Eqs. (2) and (3) are well defined; the above described layer-resolved resistivities (Eqs. (11) and (12)) are only for qualitative understanding.

Acting as an example $\Delta\rho$ is given for $s = 8$, see Fig. 4. The main contributions to $\Delta\rho$ stem from the direct interface. Some smaller contributions come from the spacer itself, but they are much smaller and nearly constant for all V thicknesses. Therefore the step of the GMR is related to changes of the interface $\Delta\rho_{\mu\mu}^k(l)$, which decreases from $0.43 \mu\Omega\text{cm}$ ($s = 4$) to $0.3 \mu\Omega\text{cm}$ ($s = 8$).

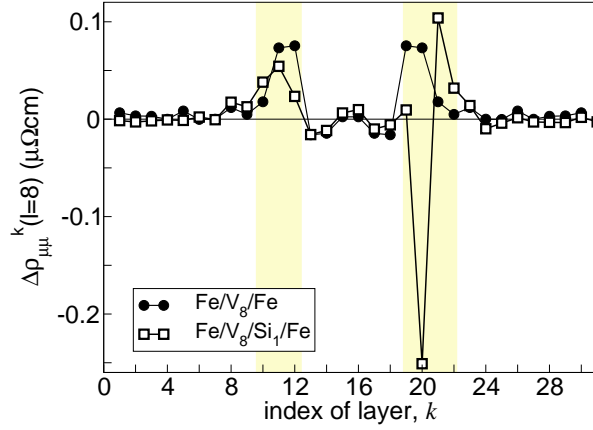


Fig. 4 Differences of the layer-resolved resistivities $\Delta\rho_{\mu\mu}^k(l)$ (Eq. (12)) for Fe/V₈/Fe (circles) and Fe/V₈/Si₁/Fe (squares) versus the layer index k . The grey shaded areas mark the interface regions.

Furthermore, it turns out that changing the scatters at the interface due to impurity layers nearly always reduces the GMR, see Fig. 3. For both geometries the reduction lies between 0.7 and 7 %, whereby in the CPP case the differences seem to vary randomly with the spacer thickness. However, in the CIP GMR the influence of the impurities vanishes with increasing V thickness i.e. the differences between the GMR values in Fig. 3 becomes smaller with increasing number of V layers. Again we can fall back on the layered resolved differences of the resistivities in Eq. (12) to discuss the reduction due to the impurity layers. An example, which is representative for the changes in the CIP GMR, is given in Fig. 4. In the case of Fe/V₈/Fe the contribution from the interfaces is large and positive. However, a Si layer at the right interface gives a very large negative $\Delta\rho_{\mu\mu}^k(l)$ (Fig. 4), which is responsible for the smaller GMR in the systems with impurities.

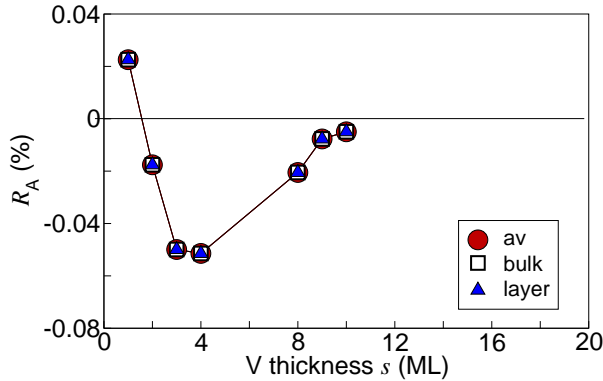


Fig. 5 AMR of Fe/V_s/Fe depending on the number of V layers s . Different symbols mark different definitions of the AMR ratio, i.e. the use of different denominators: $\rho_{||}$ (circle), bulk-like (square), layer like (triangle). For details see text.

Experimental investigations have shown that in Fe/V(110) multilayers the AMR dominates for thin V layers. Therefore, we use Eq. (8) to investigate the AMR of some particular trilayers. The AMR can be very small, i.e. we have to deal with tiny differences. To this, $\rho_{||}(C_0, l)$ and $\rho_{\perp}(C_0, l)$ have to be recalculated on a much denser k-mesh; 28185 k-points per irreducible wedge of the Brillouin zone are used. From Fig. 5 it is obvious that the AMR does not depend on the ρ_{av} (cf. Eq. (8)); all definitions give the same results up to 10^{-3} . Using a serial resistor model the AMR of Fe/V_s/Fe amounts only to $\pm 0.05\%$, which reflects at least the numerical inaccuracy. Without the use of a resistor model the AMR would be non-physically large. However, the calculated AMR is small as compared to the experimental values of $0.25 - 0.5\%$ for

Fe/V multilayers with comparable V thickness [8]. For the present systems with perfect interfaces and the magnetic moments being in-plane the AMR is negligible as compared to the GMR. This depends on the choice of the direction of the magnetic field (always in-plane) and it can be understood from the fact that no diffusion, roughness or domain structure is included in the present calculations. Experimentally the V thickness has to be larger than 17 Å until the magnetoresistance is caused by GMR and not by AMR effects [8]. Then the GMR amounts to 1–2%. As compared to the Fe/V/Fe trilayers the experimental value is somewhat smaller, i.e. for the same spacer thickness the calculated GMR is about 4.5%. This difference may also be explained by interdiffusion and roughness at the interfaces, which are not included in the present calculations. However, these suggestions are confirmed by the calculations with impurities on the V spacer (Fig. 3). For the corresponding spacer thickness s the GMR is about 2%, which is close to the experimental findings. These results have to be confirmed by further calculations including perturbations at the interfaces.

4 Conclusions

The *ab initio* calculations have confirmed that the coupling between Fe and V is short-ranged and the largest induced magnetic moment occurs at the interfaces being reduced by Al or Si layers. The impurities also reduce the GMR, up to 7% in the case of CPP geometry. Here, the magnetoresistance is always caused by the GMR; the AMR is rather small if the magnetic field is in-plane and no disorder is taken into account.

Acknowledgements Financial support was provided from the Deutsche Forschungsgemeinschaft through the SFB 491 *Structure and Transport in Magnetic Heterostructures*.

References

- [1] M. N. Baibich, J. M. Broto, A. Fert, F. N. V. Dau, F. Petroff, P. Etienne, G. Creuzet, A. Friederich, and J. Chazelas, *Phys. Rev. Lett.* **61**, 2472 (1988).
- [2] G. Binasch, P. Grünberg, F. Saurenbach, and W. Zinn, *Phys. Rev. B* **39**, 4828 (1989).
- [3] P. Weinberger, *Phys. Rep.* **377**, 281 (2003).
- [4] *Spin Dependent Transport in Magnetic Nanostructures, Advances in Condensed Matter Science*, edited by S. Maekawa and T. Shinjo (Taylor & Francis, New York, 2002).
- [5] E. Y. Tsymlal and D. G. Pettifor, *Sol. State Phys.* **56**, 113 (2001).
- [6] H. C. Herper, P. Weinberger, L. Szunyogh, C. Sommers, and P. Entel, *Phase Trans.* **76**, 523 (2003).
- [7] A. Moser, U. Krey, A. Paintner, and B. Zeller, *Magn. Mater.* **183**, 272 (1998).
- [8] P. Isberg, P. Granberg, E. Svedberg, B. Hjörvarsson, R. Wäppling, and P. Nordblad, *Phys. Rev. B* **57**, 3531 (1998).
- [9] K. Eftimova, A. Blixt, B. Hjörvarsson, R. Laiho, J. Salminen, and J. Raittila, *J. Magn. Mater.* **246**, 54 (2002).
- [10] C.-Y. You, C. H. Sowers, A. Inomata, J. S. Liang, S. D. Bader, and D. D. Koelling, *J. Appl. Phys.* **85**, 5889 (1999).
- [11] A. Broddefalk, R. Mathieu, P. Nordblad, P. Blomqvist, R. Wäppling, J. Lu, and E. Olsson, *Phys. Rev. B* **65**, 214430 (2002).
- [12] I. Turek, V. Drchal, J. Kudrnovský, M. Sôb, and P. Weinberger, *Electronic structure of disordered alloys, surfaces and interfaces* (Kluwer Academic Publisher, Dordrecht, 1997).
- [13] H. C. Herper, L. Szunyogh, P. Entel, and P. Weinberger, to be published.
- [14] H. Kronmüller, *J. Magn. Mater.* **140**, 25 (1996).
- [15] P. Weinberger, *Phil. Mag. B* **75**, 509 (1997).
- [16] P. Weinberger and L. Szunyogh, *Comp. Mater. Sci.* **17**, 414 (2000).
- [17] L. Szunyogh, B. Újfalussy, and P. Weinberger, *Phys. Rev. B* **51**, 9552 (1995).
- [18] H. Wende, A. Scherz, F. Wilhelm, and K. Baberschke, *J. Phys.: Condens. Matter* **15**, S547 (2003).
- [19] R. Kubo, *J. Phys. Soc. Jpn.* **12**, 570 (1957).
- [20] D. A. Greenwood, *Proc. Phys. Soc.* **71**, 585 (1958).
- [21] P. Weinberger, P. M. Levy, J. Banhart, L. Szunyogh, and B. Újfalussy, *J. Phys.: Cond. Matter* **8**, 7677 (1996).
- [22] H. C. Herper, *Psi-k Newsletter* **55**, 135 (2003).
- [23] P. Granberg, P. N. P. Isberg, B. Hjörvarsson, and R. Wäppling, *Phys. Rev. B* **54**, 1199 (1996).
- [24] P. M. Levy, *Solid state physics* (Academic Press, Cambridge, 1994), Vol. 47.
- [25] A. Scherz, P. Pouloupoulos, H. Wende, G. Ceballos, K. Baberschke, and F. Wilhelm, *J. Appl. Phys.* **91**, 8760 (2002).
- [26] R. Coehoorn, *J. Magn. Mater.* **151**, 341 (1995).